Low Temperature Physics/Fizika Nizkikh Temperatur, 2019, v. 45, No. 3, pp. 356–362

Rotationally induced luminescence of nanoclusters immersed in superfluid helium

P.T. McColgan[1], S. Sheludiakov[1], P.M. Rentzepis[2], D.M. Lee[1], and V.V. Khmelenko[1]

[1]*Texas A&M University, Department of Physics and Astronomy, Institute of Quantum Science and Engineering*
4242 TAMU, 77843-4242 College Station, Texas, United States
E-mail: seshel@physics.tamu.edu

[2]*Texas A&M University, Department of Electrical and Computer Engineering*
3127 TAMU, 77843-3127, College Station, Texas, United States

Received October 24, 2018

We studied the influence of rotation speed of a beaker containing superfluid helium (He II) on the intensity of luminescence of collections of nanoclusters immersed in He II. We observed an increase in the α-group emission of nitrogen atoms ($^2D \rightarrow {}^4S$ transition) in nanoclusters which correlated with the increasing of rotational speed of the beaker. Increasing luminescence was also observed by increasing the concentration of molecular nitrogen in the nitrogen-helium gas mixtures used for the formation of the molecular nitrogen nanoclusters. We suggest that this effect is caused by the change of the density of quantum vortices in He II initiated by variation of rotational speed of the beaker. When the density of the vortices is increased, the probability for the nanoclusters to become trapped in the vortex cores is also increased. The collisions in the vortex cores of trapped nanoclusters with nitrogen atoms stabilized mostly on the surfaces of the nanoclusters initiate the recombination of nitrogen atoms resulting in luminescence.

Keywords: luminescence, quantized vortices, optical spectroscopy, nanoclusters.

1. Introduction

Fascination with quantum vortices in superfluid helium (He II) started with their discovery in the 1950s, and continues today [1]. Investigations of quantum vortices in superfluid helium have recently attracted great attention [2–4]. The visualization of vortex cores [1] has led to the observation of the reconnection of vortices and direct observation of Kelvin waves excited by quantized vortex reconnections [5,6], characterization of the probability density function representing particle velocity [7] and acceleration in thermal counterflow [8]. Metastable helium molecules were used as tracers in superfluid helium [9], providing the possibility for studying quantum turbulence in He in the $T = 0$ limit [10] and examine the normal fluid behavior in thermal counterflow [11,12]. The technique of nanowire formation by ablating metallic nanoparticles from a target in He II was realized on the basis of coalescence of the nanoparticles in the vortex cores [13,14]. The luminescence of ensembles of molecular nitrogen nanoclusters containing stabilized nitrogen atoms was initiated in He II by quantum vortices [15]. In this latter case the dependence of luminescence intensity on temperature was correlated with that of the vortex density in the temperature range 1.2–2.1 K. These nanoclusters are created by the injection of nitrogen-helium gas mixtures into bulk He II after passing through a radio-frequency discharge zone [16].

In this work we studied the influence of vortex density in He II on the intensity of luminescence accompanied by the process of injection of molecular nitrogen nanoclusters into a rotating beaker with He II. During these measurements, the nanoclusters continued to enter into the bulk He II inside the rotating beaker. Nitrogen atoms stabilized on the surfaces of nanoclusters [17] provide an excellent opportunity for visualization of the process of capturing nanoclusters into vortex cores. When two nanoclusters are captured into a vortex core, they can collide and two nitrogen atoms residing on the surfaces of these nanoclusters can then recombine, starting processes which lead to luminescence of nitrogen atoms in nanoclusters. We observed the influence of rotation speed of the beaker with He II on the intensity of luminescence from the ensembles of nanoclusters.

We found that increasing the rotation speed of the beaker with He II led to an increase in luminescence of the injected nanoclusters. We explained this effect by an efficient capturing of nanoclusters in quantum vortex cores when the density of vortices was increased. Increasing the

density of vortices with increasing the rotational speed of the beaker with He II results in more chemical reactions of pairs of nitrogen atoms on the surfaces of neighboring nanoclusters in vortex cores leading to increasing the intensity of luminescence.

2. Experimental setup

Our experimental setup contains two concentric glass Dewars. The inner Dewar is filled with liquid helium, the outer Dewar with liquid nitrogen. The inner Dewar is pumped with an Edwards model 80 vacuum pump, achieving liquid helium temperatures as low as 1.1 K.

The top flange of the cryogenic system houses all of the connections to room-temperature equipment, including a vacuum feed-through for our cryogenic fiber assembly, and a vacuum feed-through for all electrical connections.

Gas mixtures are prepared at room temperature using a gas handling system. This system consists of a manifold connecting pressurized gas cylinders to mixing tanks, a pressure gauge and connections to the cryostat and a vacuum pump. The flow of the gas mixture to the cryostat is regulated by a Brooks Model 5850 flux controller.

Samples are created by passing a gas mixture through an atomic source. The atomic source consists of a stainless steel vacuum jacket housing a quartz discharge tube. The discharge tube is made of an outer quartz tube with a concentric quartz capillary. At the bottom of the quartz capillary there are electrodes for a radio-frequency (RF) discharge. The RF discharge is provided by a HP 8656B signal generator amplified by an E&I 3100L. The outer quartz tube is filled with liquid nitrogen (LN_2) which simultaneously cools the incoming gas mixture in the capillary, and the discharge electrodes.

After passing through the RF discharge zone, excited atoms and molecules exit the orifice, diameter 0.75 mm, of the quartz capillary. The pressure gradient ~2 Torr between the discharge zone and the cryostat creates a well-formed jet of discharge products which is injected into the beaker filled with superfluid helium (He II). The level of the He II in the beaker is maintained constant (22 mm below the orifice) using a thermo-mechanical (fountain-effect) pump. The temperature during sample preparation (T ~ 1.54 K) is measured using a germanium thermometer.

One unique feature of this setup is the ability to rotate our beaker at cryogenic temperatures. The possibility of rotating a beaker containing He II was demonstrated in previous work [18,19]. In our setup, rotation of the beaker is accomplished by mounting the quartz beaker to the output shaft of a stepper motor (see Fig. 1). The quartz beaker sits in a teflon holder which is attached to a brass flange with screws. The brass flange is secured to the output shaft of the stepper motor with a set screw.

The electric motor is powered by a 24 VDC power supply controlled by a stepper motor driver and an Arduino microcontroller. The Arduino microcontroller is running a program which enables the motor, controls the direction of rotation, and "ramps up" the rotational speed from zero to the desired speed, as well as displaying this speed on a seven-segment display. The Arduino microcontroller provides a chain of TTL pulses to the DM320T stepper motor driver. This driver has built-in current limiting capabilities, which reduces heating inside the stepper motor coils, as well as providing the microstepping. These are controlled by dip-switches located on the side of the stepper motor driver.

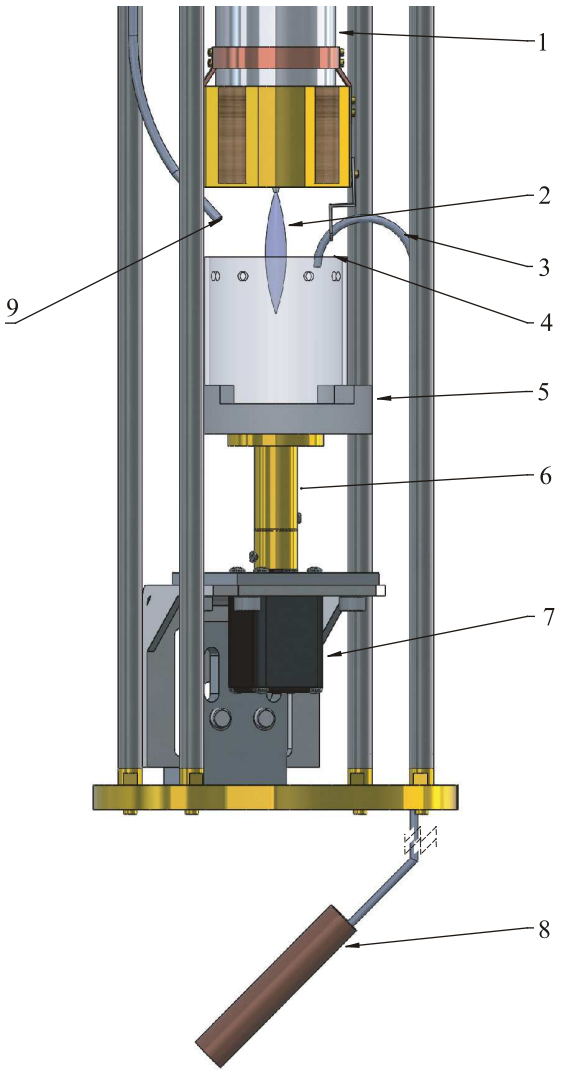

Fig. 1. Rotating beaker assembly: atomic source (1), nitrogen-helium jet (2), fountain pump line (3), quartz beaker (4), teflon beaker holder (5), brass flange (6), NEMA 8 stepper motor (7), fountain pump body (8), optical fiber (9).

The motor is a standard NEMA 8 motor with 200 steps per revolution, or 1.8 deg. per step. With the microstepping from the driver, there are a total of 1600 microsteps per revolution (13.5 arcmin per microstep). Each TTL pulse from the microcontroller advances the motor one step. The use of microstepping allows for smoother rotation of the beaker.

The motor itself is an off-the shelf part, which was modified to perform in cryogenic conditions. The two bearings connected to the rotor were removed and thoroughly cleaned using an aerosol solvent. This solvent is generally used to remove oil and debris from automotive sensors, and it is safe for sensitive electronics. The liquid oil lubricants would be frozen at cryogenic temperatures. The bearings were then lubricated using a molybdenum disulfide (MbS_2) dry lubricant applied with an aerosol solvent. After application, the solvent is evaporated, leaving a thin film of dry MbS_2.

The operation of the motor provided an additional heat load so that all experiments were performed at a slightly elevated temperatures 1.53–1.54 K compared to the optimal condition ($T = 1.5$ K).

The emission of the ultraviolet (UV) and visible (VIS) light is collected using a cryogenic fiber assembly which terminates at a vacuum-tight optical feed-through on the top flange. A bifurcated optical fiber connects this feed-through to the Andor Shamrock 500i and Ocean Optics HR2000+ spectrometers. The emission of the near-infrared (NIR) light is collected through the slits in the silvering of the Dewars by a focusing lens located outside of the Dewars, onto the entrance of a collimating lens mounted at the end of an optical fiber connected to an Avantes NIR 512-1.7 TEC spectrometer.

We recorded the luminescence during the injection of the products of a discharge in nitrogen-helium gas mixtures into bulk superfluid helium contained in the cylindrical quartz beaker (see Fig. 1). During these recordings the beaker was rotated at various speeds. The rotation speeds were equal to 3, 4, and 7.5 rad/s. These speeds were similar to those used for measurements of the attenuation of second sound in uniformly rotating He II [18]. For each rotation speed the recording of luminescence lasted for 5 minutes. We performed investigations for three different nitrogen-helium gas mixtures: N_2:He = 1:400, 1:200, and 1:100.

3. Experimental results

We recorded the luminescence spectra and their intensity during the injection of nanoclusters into bulk superfluid helium while the beaker with helium was rotating uniformly. The spectra were obtained over a broad range. The Ocean Optics spectrometer provided spectra in the 200–1100 nm range, the Andor spectrometer in 240–480 nm range, and the Avantes spectrometer in the 900–1700 nm range.

Figure 2 shows the spectra obtained by the Andor spectrometer during the condensation of gas mixture N_2:He = = 1:200 for three different rotational speeds of the beaker filled with He II. From the comparison of these spectra one can see that the intensities of emission assigned to the molecular nitrogen bands and helium atomic lines which were collected from the gas phase jet are almost the same for all three rotation speeds of the beaker.

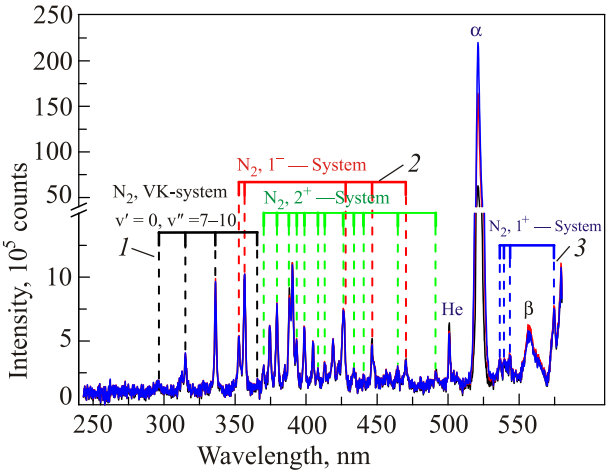

Fig. 2. (Color online) Spectra observed with the Andor spectrometer during condensation of the mixture N_2:He = 1:100 and 1:200 into a beaker filled with He II for different rotational speeds: 3 rad/s (black, *1*), 4 rad/s (red, *2*), 7.5 rad/s (blue, *3*). Each spectrum was obtained by integration of the emission during a 5 minute time interval.

In contrast, the α-group emission of nitrogen atoms in nanoclusters immersed into superfluid helium depends on the rotation speed of the beaker with He II. Increasing the rotation speed of the beaker from 3 rad/s to 7.5 rad/s resulted in a substantial increase of the α-group emission. Figure 3 shows a comparison of intensities of α-group emission during the injection of two different gas mixtures (N_2:He = 1:100 and 1:200) for three different rotational speeds of the beaker filled with liquid helium. These spectra were obtained by the Andor spectrometer using the first grating with a resolution of 0.5 nm.

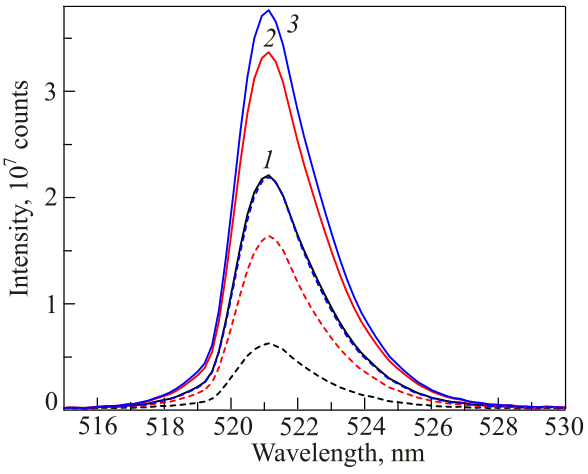

Fig. 3. (Color online) Comparison of α-group emission observed during condensation of gas mixtures N_2:He = 1:100 (solid line) and 1:200 (dashed line) for different rotational speeds: 3 rad/s (black, *1*), 4 rad/s (red, *2*), 7.5 rad/s (blue, *3*). Each spectrum was obtained by integration of the emission during a 5 minute time interval.

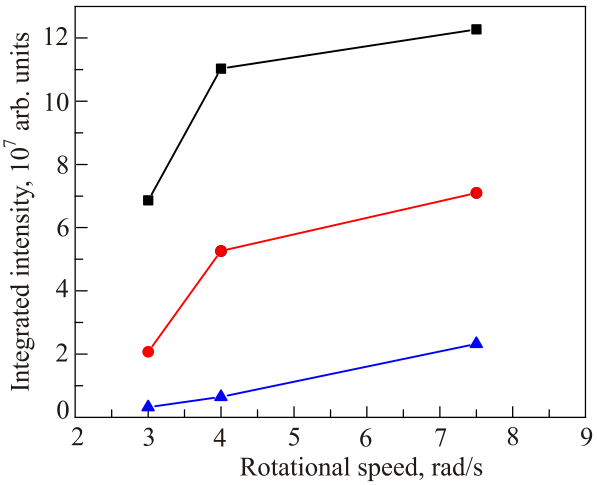

Fig. 4. (Color online) Dependence of integrated intensity of N atom α-group observed during the injection of nitrogen-helium gas mixtures N_2:He = 1:100 (black squares), 1:200 (red circles) and 1:400 (blue triangles) into a rotating beaker with He II on the rotation speed of the beaker.

We performed similar investigations for the gas mixture N_2:He = 1:400. Fig. 4 shows the dependence of integrated intensity of the α-group of N atoms in nanoclusters immersed into He II on the rotation speed of the beaker for three different gas mixtures used for injection of nanoclusters. It is clearly seen that increasing the rotational speed of the beaker led to an increase of the integrated luminescence for each of the gas mixtures used in the experiments. Also, it was found that increasing the flux of nitrogen clusters into bulk He II resulted in increasing the intensity of the α-group for each value of rotation speed of the beaker.

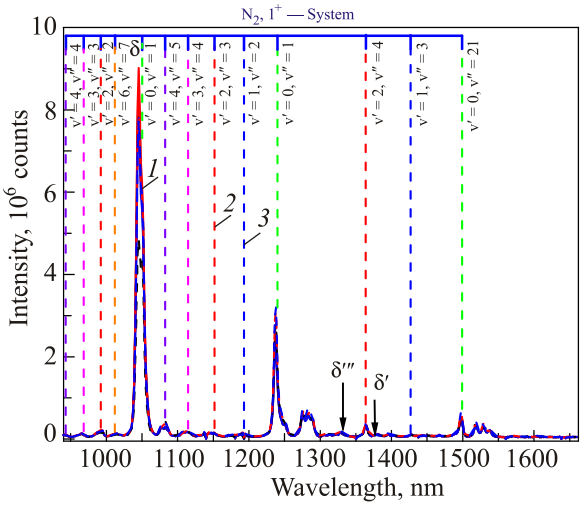

Fig. 5. (Color online) Comparison of the spectra in the range 900–1650 nm observed with the Avantes spectrometer during the injection of nitrogen-helium gas mixture N_2:He = 1:100 (solid line) and 1:200 (dashed line) into a rotating beaker with He II for different rotational speeds: 3 rad/s (black, *1*), 4 rad/s (red, *2*), 7.5 rad/s (blue, *3*).

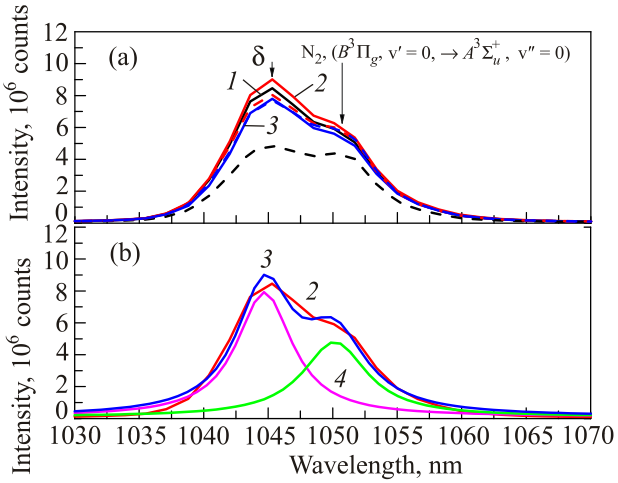

Fig. 6. (Color online) (a) Comparison of the spectra of overlapping N atom δ-group and N_2 ($B^3\Pi_g$, $v' = 0 \rightarrow A^3\Sigma_u^+$, $v'' = 0$) emissions observed during the injection of nitrogen-helium gas mixtures N_2:He = 1:100 (solid lines) and 1:200 (dashed lines) into rotating He II for different rotational speeds: 3 rad/s (black, *1*), 4 rad/s (red, *2*), 7.5 rad/s (blue, *3*). (b) Deconvolution of the overlapping spectra of δ-group and N_2 ($B^3\Pi_g$, $v' = 0 \rightarrow A^3\Sigma_u^+$, $v'' = 0$) emissions. Experimental spectrum of these two bands recorded during injection of N_2:He = 1:100 gas mixture into beaker rotating at 4 rad/s (red, *2*), Lorentzian fitting line for δ-group emission (magenta), Lorentzian fitting line for N_2 ($B^3\Pi_g$, $v' = 0 \rightarrow A^3\Sigma_u^+$, $v'' = 0$) emission (green, *4*), the sum of the fitting lines (blue, *3*).

The spectra observed in the NIR range by the Avantes spectrometer show a result similar to that obtained in the UV–VIS ranges, namely, the emission from the gas-phase jet was essentially unaltered by the rotation of the beaker with He II as seen in Fig. 5. The most dramatic effect of rotating He II was observed for the emission of the δ-group of N atoms stabilized in the N_2 nanoclusters. Figure 6(a) shows a comparison of the intensities of the overlapping N atom δ-group and N_2 ($B^3\Pi_g$, $v' = 0 \rightarrow A^3\Sigma_u^+$, $v'' = 0$) emissions during the injection of two different gas mixtures (N_2:He = 1:100 and 1:200) for three different rotational speeds of the beaker. Similar investigations were made for gas mixture N_2:He = 1:400. We performed deconvolution for these overlapping bands. An example of the analysis is shown in Fig. 6(b) for the spectra recorded during the injection of N_2:He 1:100 gas mixture into the beaker rotating with the angular speed 4 rad/s. A similar deconvolution was made for all spectra shown in Fig. 6(a) to obtain the dependence of the integrated intensity of δ-group emission on the rotation speed of the beaker. Figure 7 shows the dependence of the integrated intensity of the N atom δ-group in nanoclusters immersed in He II on the rotational speed of the beaker with He II for three different gas mixtures used for injection of nanoclusters. For gas mixture 1:400 an almost linear growth of the δ-group intensity with increasing rotational speed of He II was observed. For more concentrated

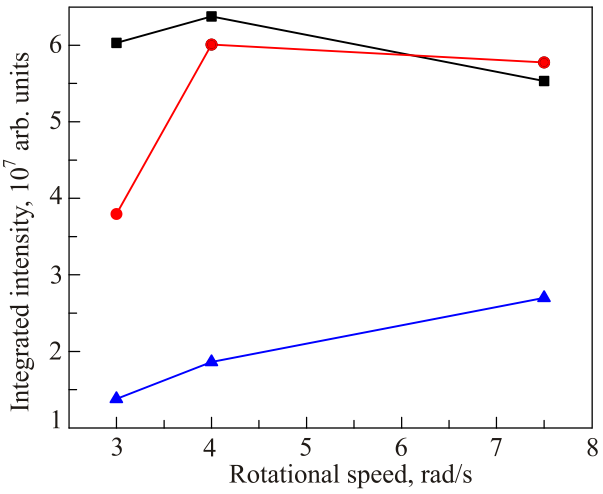

Fig. 7. (Color online) Dependence of integrated intensity of N atom δ-group observed during the injection of nitrogen-helium gas mixtures N_2 = 1:100 (black squares), 1:200 (red circles), 1:400 (blue triangles) into He II on the rotation speed of the beaker. Integrated intensities of δ-group lines were obtained from the deconvolution of the spectra shown in Fig. 6(a).

gas mixtures N_2:He = 1:100 and 1:200 increasing of the integrated intensity of δ-group was observed only with increasing the rotation speed of the beaker from 3 to 4 rad/s. Further increase of the rotational speed of the beaker with He II to 7.5 rad/s resulted in a small decrease of the intensity of δ-group emission.

4. Discussion

Superfluid helium is characterized by two unique features, anomalously high heat conductance and formation of quantized vortices. The efficient heat removal property of He II was efficiently used in the method of injection of products of our discharge in nitrogen-helium gas mixtures into bulk He II [16]. This approach allows us to achieve the highest concentrations of stabilized nitrogen atoms [20–22]. Nitrogen atoms are stabilized on molecular nitrogen nanoclusters, which form an aerogel-like porous structure inside He II [23]. Nanoclusters are formed during the process of cooling down atoms and molecules entering from the gas discharge zone by passage through the cold helium vapors on the way to the surface of He II in the collection beaker. From *x*-ray investigations of nanoclusters collected inside He II an estimate of the average size of nanoclusters on the order of 5 nm has been made [24,25]. This allows us to determine the flux of nanoclusters to be $2\cdot10^{13}$ s^{-1} in the process of condensation of our nitrogen-helium gas mixture N_2:He = 1:100 which has a flux 10^{19} s^{-1}. Each nanocluster contains on average 50 nitrogen atoms, which reside mostly on the surfaces of these nanoclusters [17]. Usually during the process of their injection into He II, the nanoclusters collide inside superfluid helium and nitrogen atoms from the adjacent nanocluster strands can meet each other and recombine. This leads to continuous luminescence from nanoclusters inside He II. As a result of N atom recombination, the N_2 molecules in high vibrational states are formed. The recombination energy (~9.8 eV) is released rather slowly in the time scale of a few seconds [26,27]. This time scale allows the removal of heat released from the nanoclusters during the process of vibrational relaxation of excited N_2 molecules by the high heat conductance of superfluid helium [28]. Another part of the N_2 molecule excitation transfers efficiently to the stabilized atoms and is subsequently released by light emission. These two processes prevent the thermal explosions of nanoclusters [29]. As a consequence the ensembles of molecular nitrogen nanoclusters with high concentrations of nitrogen atoms are stable upon immersion into superfluid helium. The mechanism of thermoluminescence in solid nitrogen containing stabilized nitrogen atoms is well understood [30–32]. Two ground state nitrogen atoms recombine to form metastable nitrogen molecules.

$$N(^4S) + N(^4S) \rightarrow N_2(A^3\Sigma_u^+)\,. \qquad (1)$$

Energy from these molecules can be transferred to ground state nitrogen atoms stabilized in the nanoclusters.

$$N_2(A^3\Sigma_u^+) + N(^4S) \rightarrow N(^2D) + N_2(X^1\Sigma_u^+)\,. \qquad (2)$$

These excited $N(^2D)$ nitrogen atoms emit the α-group.

$$N(^2D) \rightarrow N(^4S) + \alpha\text{-group}. \qquad (3)$$

Similarly for the δ-group, metastable nitrogen molecules can excite stabilized nitrogen atoms, to the higher $N(^2P)$ metastable state.

$$N_2(A^3\Sigma_u^+) + N(^4S) \rightarrow N(^2P) + N_2(X^1\Sigma_u^+) \qquad (4)$$

which emit the δ-group

$$N(^2P) \rightarrow N(^4D) + \delta\text{-group}. \qquad (5)$$

In this work we studied the influence of the rotation speed of the beaker with He II on the intensity of luminescence of nitrogen atoms in the process of injecting nanoclusters into rotating He II. It was found experimentally (see Figs. 2 and 3) that rotation of the beaker with He II substantially increases the intensity of luminescence of nitrogen atoms in molecular nitrogen nanoclusters immersed in He II. Increasing the rotation speed of the beaker with He II from 3 rad/s to 7 rad/s led to 1.5–6 fold increase of α-group intensity for the gas mixtures studied. When we increased the flux of nanoclusters by changing gas mixture from N_2:He = = 1:400 to gas mixture N_2:He =1:100 the intensity of luminescence from nanoclusters in rotating He II also increased for each of the three rotation speeds investigated as seen in Fig. 7. In our earlier work we found that applying temperature gradients to the collection of nanoclusters immersed in He II led to the initiation of chemical reactions of nitrogen

atoms stored on the surfaces of the nanoclusters [15]. The luminescence of ensembles of nanoclusters immersed in He II was found to be correlated with the vortex density in bulk He II. This correlation was explained by using a model, which suggested that some loose nanoclusters were captured in the vortex cores in He II. Inside the vortex cores nanoclusters collide more efficiently and the recombination of nitrogen atoms residing on surfaces of nanoclusters was initiated. As a result of nitrogen atom recombination and other processes described above, nitrogen atom luminescence was observed. The intensity of this luminescence thus tended to increase with the density of vortices in the He II.

We follow the same model to explain the results obtained in this work, only the method of forming vortices is more straightforward. By rotating our beaker containing He II we created an array of quantum vortices, which aligned parallel to the axis of the beaker corresponding to the direction of the injected flux of nanoclusters entering bulk He II. When nanoclusters enter into bulk He II, they introduce a heat flux, which is compensated by the superfluid component of He II. The superfluid component moves to the location of the entering nanoclusters, while simultaneously the normal component of helium moves in the opposite direction. Nanoclusters can move together with the normal component of helium. Thus nanoclusters can be captured in vortex cores. Increasing vortex density by rotation of the beaker should increase the efficiency for capturing nanoclusters into the array of vortex cores. Inside the vortex cores the collision rate of nanoclusters becomes larger [14]. Collisions of pairs of nanoclusters can lead to recombination of nitrogen atoms residing on their surfaces. As a result, rotation of the beaker can initiate chemical reactions between nitrogen atoms in the vortex cores, leading to formation of highly excited nitrogen molecules. The energy from excited nitrogen molecules was efficiently transferred to stabilized nitrogen atoms, which was responsible for the increased luminescence.

The density of the quantized vortices in He II, L, is given by the Feynman rules with $L = 2000\ \Omega\cdot\text{cm}^{-2}$, where Ω is the angular velocity of the beaker in rad/s. The observed increase in the intensity of N atom luminescence when rotation speed of He II was increased from 3 to 7.5 rad/s can be explained by the proportional increase of the vortex density from 6000 cm^{-2} to 15000 cm^{-2}.

The increase in the intensity of luminescence for each rotation speed of the beaker with He II when the content of N_2 molecules in the condensed gas mixtures was increased can be explained by an increase of the flux of nanocluster participating in chemical reactions in the vortex cores. The model works well for explaining the behavior of the α-group emission of N atoms in nanoclusters injected into a rotating beaker with He II.

The behavior of δ-group emission of N atoms is similar at low rotation speeds of He II, but at higher rotation speed (7.5 rad/s) the intensity of δ-group emission was saturated (see Fig. 7). To understand the latter result, additional investigations are needed. It may be that differences in the behavior of α-group and δ-group emissions are somehow connected to differences in the lifetimes of the ^2D and ^2P states of nitrogen atoms in the N_2 solid matrix, which are equal to 30 s and 1 ms, respectively, or related to differences in the formation of these metastable states of N atoms.

5. Conclusions

1. We observed direct correlation between the increase of rotation speed of the beaker with He II and the increase of luminescence intensity of N atom α-group in molecular nitrogen nanoclusters during their injection into a rotating beaker with He II. The increase of the luminescence intensity with increasing He II rotation speed was explained by the initiation of chemical reactions of N atoms on the surfaces of nanoclusters trapped inside vortex cores. Increasing the rotation speed of He II led to an increase of the vortex density and, correspondingly, an enhancement of the processes of chemical reactions involving trapped nanoclusters in the vortex cores.

2. The method of initiation of luminescence of nitrogen nanoclusters immersed in He II can be used to visualize vortex cores and to study quantum turbulence in He II.

3. This method opens the possibility of initiating chemical reactions for a variety of free radicals residing on the surfaces of nanoclusters immersed in bulk He II. It may also provide new possibilities for synthesis of exotic new species.

Acknowledgments

This work has been supported by the NSF grant number # DMR 1707565, the ONR Award N00014-16-1-3054 and AFOSR grant #FA9550-18-0100.

1. G.P Bewley, D.P. Lathrop, and K.R. Sreenivasan, *Nature* **441**, 588 (2006).
2. W.F. Vinen, *J. Low Temp. Phys*. **145**, 7 (2006).
3. C.F. Barenghi, L. Skrbek, and K.R. Sreenivasan, *Proc. Natl. Acad. Sci. USA,* (*Suppl. 1*) **111**, 4647 (2014).
4. Y.A. Sergeev and C.F. Barenghi, *J. Low Temp. Phys*. **157**, 429 (2009).
5. G.P. Bewley, M.S. Paoletti, K.R. Sreenivasan, and D.P. Lathrop, *Proc. Natl. Acad. Sci. USA* **105**, 13707 (2008).
6. E. Fonda, D.P. Meichle, N.T. Ouellette, S. Hormoz, and D.P. Lathrop, *Proc. Natl. Acad. Sci. USA,* (*Suppl. 1*) **111**, 4707 (2014).
7. M.S. Paoletti, M.E. Fisher, K.R. Sreenivasan, and D.P. Lathrop, *Phys. Rev. Lett*. **101**, 154501 (2008).
8. M.La Mantia, D. Duda, M. Rotter, and L. Skrbek, *J. Fluid Mech*. **717**, R9 (2013).
9. W. Guo, J.D. Wright, S.B. Cahn, J.A. Nikkel, and D.N. McKinsey, *Phys. Rev. Lett.* **102**, 235301 (2009).
10. D.E. Zmeev, F. Pakpour, P.M. Walmsley, A.I. Golov, W. Guo, D.N. McKinsey, G.G. Ihas, P.V.E. McClintock,

S.N. Fisher, and W.F. Vinen, *Phys. Rev. Lett.* **110**, 175303 (2013).
11. W. Guo, S.B. Cahn, J.A. Nikkel, W.F. Vinen, and D.N. McKinsey, *Phys. Rev. Lett*. **105**, 045301 (2010).
12. W. Guo, M. La Mantia, D.P. Lathrop, and S.W. Van Sciver, *Proc. Natl. Acad. Sci.* **111**, 4653 (2014).
13. E.B. Gordon, A.V. Karabulin, V.I. Matyushenko, V.D. Sizov, and I.I. Khodos, *J. Exp. Theor. Phys.* **112**, 1061 (2011).
14. E.B. Gordon, A.V. Karabulin, V.I. Matyushenko, V.D. Sizov, and I.I. Khodos, *Chem. Phys. Lett*. **519-520**, 64 (2012).
15. A. Meraki, P.T. McColgan, P.M. Rentzepis, R.Z. Li, D.M. Lee, and V.V. Khmelenko, *Phys. Rev. B* **95,** 104502 (2017).
16. E.B. Gordon, L.P. Mezhov-Deglin, and O.F. Pugachev, *J. Exp. Theor. Phys. Lett.* **19,** 63 (1974).
17. S. Mao, R.E. Boltnev, V.V. Khmelenko, and D.M. Lee, *Fiz. Nizk. Temp*. **38**, 1313 (2012) [*Low Temp. Phys*. **38**, 1037 (2012)].
18. H.E. Hall and W.F. Vinen. *Proc. Roy. Soc. London A* **238**, 204 (1956).
19. E.B. Gordon, M.I. Kulish, A.V. Karabulin, V.I. Matyushenko, E.V. Dyatlova, A.S. Gordienko, and M.E. Stepanov, *Fiz. Nizk. Temp*. **43**, 1316 (2017) [*Low Temp. Phys*. **43**, 1055 (2017)].
20. E.B. Gordon, V.V. Khmelenko, A.A. Pelmenev, E.A. Popov, and O.F. Pugachev, *Chem. Phys. Lett*. **155**, 301 (1989).
21. R.E. Boltnev, I.N. Krushinskaya, A.A. Pelmenev, E.A. Popov, D.Yu. Stolyarov, and V.V. Khmelenko, *Fiz. Nizk. Temp*. **31**, 723 (2005) [*Low Temp. Phys*. **31**, 547 (2005)].
22. E.P. Bernard, R.E. Boltnev, V.V. Khmelenko, and D.M. Lee, *J. Low Temp. Phys*. **134**, 199 (2004).
23. S.I. Kiselev, V.V. Khmelenko, D.M. Lee, V. Kiryukhin, R.E. Boltnev, E.B. Gordon, and B. Keimer, *Phys. Rev. B* **65**, 024517 (2001).
24. V. Kiryukhin, B. Keimer, R.E. Boltnev, V.V. Khmelenko, and E.B. Gordon, *Phys. Rev. Lett*. **79**, 1774 (1997).
25. V. Kiryukhin, E.P. Bernard, V.V. Khmelenko, R.E. Boltnev, N.V. Krainyukova, and D.M. Lee, *Phys. Rev. Lett*. **98**, 195506 (2007).
26. A.A. Ovchinnikov, *Sov. Phys. J. Exp. Teor. Phys.* **30**, 147 (1970).
27. K. Dressler, O. Oehler, and D.A. Smith, *Phys. Rev. Lett*. **34**, 1364 (1975).
28. V. Arp, *Cryogenics* **10**, 96 (1970).
29. E.B. Gordon, L.P. Mezhov-Deglin, O.F. Pugachev, and V.V. Khmelenko, *Sov. Phys. J. Exp. Teor. Phys.* **46**, 502 (1977).
30. A.M. Bass and H.P. Broida, *Formation and Trapping of Free Radicals*, Academic Press, New York, London (1960).
31. O. Oehler, D. A. Smith, and K. Dressler, *J. Chem. Phys.* **66**, 2097 (1977).
32. A. Meraki, S. Mao, P.T. McColgan, R.E. Boltnev, D.M. Lee, and V.V. Khmelenko, *J. Low Temp. Phys.* **185**, 269 (2016).

Індукована обертанням люмінесценція нанокластерів, які знаходяться у надплинному гелії

P.T. McColgan, S. Sheludiakov, P.M. Rentzepis, D.M. Lee, and V.V. Khmelenko

Досліджено вплив швидкості обертання склянки з надплинним гелієм (He II) на інтенсивність люмінесценції нанокластерів, які знаходяться всередині He II. Спостерігається збільшення емісії α-групи атомів азоту (перехід $^2D \rightarrow {}^4S$) в нанокластерах, яке корелювало зі збільшенням швидкості обертання склянки. Збільшення люмінесценції також спостерігалося при збільшенні вмісту молекулярного азоту в азотно-гелієвій газовій суміші, яку використовували для отримання нанокластерів молекулярного азоту. Ми припускаємо, що цей ефект пов'язаний зі зміною щільності квантових вихорів в He II при зміні швидкості обертання склянки. При збільшенні щільності вихорів, ймовірність захоплення нанокластеров в серцевинах вихорів також підвищується. Усередині серцевин вихорів відбувається зіткнення нанокластерів, внаслідок цього відбувається рекомбінація атомів азоту, що знаходяться на поверхні нанокластерів, та їх люмінесценція.

Ключові слова: люмінесценція, квантові вихори, оптична спектроскопія, нанокластери.

Индуцированная вращением люминесценция нанокластеров, находящихся в сверхтекучем гелии

P.T. McColgan, S. Sheludiakov, P.M. Rentzepis, D.M. Lee, and V.V. Khmelenko

Исследовано влияние скорости вращения стакана со сверхтекучим гелием (He II) на интенсивность люминесценции нанокластеров, находящихся внутри He II. Наблюдается увеличение эмиссии α-группы атомов азота (переход $^2D \rightarrow {}^4S$) в нанокластерах, которое коррелировало с увеличением скорости вращения стакана. Увеличение люминесценции также наблюдалось при повышении содержания молекулярного азота в азотно-гелиевой газовой смеси, используемой для получения нанокластеров молекулярного азота. Мы предполагаем, что этот эффект связан с изменением плотности квантовых вихрей в He II при изменении скорости вращения стакана. При увеличении плотности вихрей, вероятность захвата нанокластеров в сердцевинах вихрей также увеличивается. Внутри сердцевин вихрей происходит столкновение нанокластеров, в результате которого происходит рекомбинация атомов азота, находящихся на поверхности нанокластеров, и их люминесценция.

Ключевые слова: люминесценция, квантовые вихри, оптическая спектроскопия, нанокластеры.